Precision Relative Astrometry with the Deep Space Network

W. A. Majid[1] and D. S. Bagri[1]

We report here results of single-baseline very long baseline interferometry (VLBI) observations of pairs of quasars, carried out at 8.4 GHz on the Madrid–Goldstone baseline with Deep Space Network (DSN) 34-m antennas. Using a fast-switching technique, we are able to successfully carry out phase connection for each observation, resulting in relative astrometric precision of a few picoseconds, equivalent to an angular precision of ∼0.2 nanoradians. In this article, we will discuss the potential of phase delay observations and the technique used to reliably connect phase across observations of calibrator and program source. We will show that by reducing both the temporal and angular separation between the calibrator and program source (either a natural radio source or a spacecraft) we are able to minimize and cancel many sources of common mode error, such as media variations and instrumental changes, as well as errors associated with lack of knowledge of the exact observing geometry. We also will discuss the implications of these results for potential gains in improved accuracy for measurements of spacecraft angular position at the DSN.

I. Introduction

There are a number of factors that limit the accuracy of spacecraft angular position measurements using very long baseline interferometry (VLBI). VLBI determines the relative angular position of a spacecraft with respect to a compact calibration radio source (normally a quasar). Obtaining the absolute position measurement of the spacecraft requires knowledge of the position of the reference source. The position of the reference source typically is well determined by making multiple measurements prior to observation of the spacecraft. The reference source either is part of an all-sky catalog, which is maintained to high precision through routine catalog observations, or can be chosen in a region of interest, e.g., near Mars during an orbit insertion event. In the latter case, the reference source is observed multiple times prior to a critical event, and its position is determined accurately relative to a stable all-sky catalog, such as the International Celestial Reference Frame (ICRF) catalog. In either case, however, it is evident that the accuracy of the absolute measurement of the angular position of a spacecraft is dependent on the accuracy of the all-sky reference catalog.

Other factors affecting the precision of astrometric measurements, apart from measurement of signal-to-noise ratio (SNR), are variations in propagation path length for the signals arriving at the VLBI

[1] Tracking Systems and Applications Section.

The research described in this publication was carried out by the Jet Propulsion Laboratory, California Institute of Technology, under a contract with the National Aeronautics and Space Administration.

antennas due to temporal and spatial separation between the measurements of the reference source and the target source (e.g., spacecraft), instrumental changes, and knowledge of the observing geometry (like Earth orientation, location of the VLBI antennas and their axes of rotations, etc). To achieve good measurement accuracy, a trade-off is made between SNR, angular separation between calibrator and target, and integration time for the observations. The SNR for measurements on a calibration reference source depends on the strength (flux density) of suitable available sources for calibration and on the integration time. These in turn determine the angular separation between the calibrator and spacecraft and the integration time to achieve reasonable measurement accuracy.

Many components contributing to calibration errors are linearly proportional to the temporal and angular separation between the reference calibrator and target source. Therefore, it is expected that, by reducing the temporal and angular separation between the calibrator and the target, we will minimize the effects of propagation variations, instrumental changes, and lack of knowledge of the exact observing geometry. The temporal separation can be reduced by using many short interleaved observations of the spacecraft and calibrator and still accumulate enough total SNR by making as many measurement cycles as necessary to provide the required overall integration time. Of course, the minimum cycle time has to be balanced against practical considerations like the amount of time elapsed in moving the antennas from one source to another and the settling time required for starting the measurements when antennas are moved. To assess the degree of improvements that can be achieved by reducing the angular and temporal separation, we have carried out VLBI pilot observations of several pairs of quasars separated by 1 to 2 deg on sky using DSN 34-m antennas at 8.4 GHz (X-band). The switching cycle time was 1 to 2 minutes between observations of the calibrator and the target source (another quasar in this case).

The organization of this article is as follows: In Section II, a brief theoretical background with a description of VLBI relative measurements and group versus phase delay is given; Section III discusses the expected error budget for fast-switching measurements; Sections IV and V describe the selection of quasar pairs and DSN observations,respectively; Section VI provides a detailed discussion of VLBI data reduction; Section VII describes the results from each set of observatons; Section VIII includes a discussion of the application of these techniques for measuring spacecraft angular position as well as future improvements and limitations; and finally, in Section IX we conclude with a summary of our findings.

II. Theory

VLBI measures the fringe phase of the visibility function, $A\cos(\phi)$, with $\phi \sim 2\pi\nu\tau$, where A is the fringe amplitude, ϕ is the fringe phase, ν is the observing frequency, and τ is the delay (time difference) in the arrival of electromagnetic waves at two widely separated antennas. The fringe phase depends on the source-baseline geometry, propagation media, and instrumental effects:

$$\phi(t) \simeq (2\pi\nu B/c)[\cos D \cos\delta \cos(A_\circ + \Omega t - \alpha) + \sin D \sin\delta] + \phi_{\rm prop}(t) + \phi_{\rm inst}(t) + \phi_{\rm str} + 2\pi n \qquad (1)$$

where B is the length of the baseline; c is the speed of light; $A_\circ$ and D are the right ascension at epoch and declination of the baseline, respectively; α and δ are the source right ascension and declination, respectively; Ω is the magnitude of the angular velocity of the Earth; $\phi_{\rm prop}$, $\phi_{\rm inst}$, and $\phi_{\rm str}$ are contributions from the propagation medium, instrumentation, and source structure, respectively; and n is an integer. The last term in the above equation indicates the integer cycle (2π) ambiguity of the phase observable.

If we observe a second source near the reference source in angular position, and if the two observations are made at the same time, the difference in phase can be used to provide an estimate of the offset in angular position of one source with respect to the other. For instance, if the second source has right ascension and declination given by $\alpha + \Delta\alpha$ and $\delta + \Delta\delta$, respectively, then the phase difference may be approximated to first order in position offset by

$$\Delta\phi(t) \simeq (2\pi\nu B/c)\left[\Delta\alpha\,\cos D\,\cos\delta\,\sin(A_\circ + \Omega t - \alpha)\right.$$

$$-\,\Delta\delta\,\cos D\,\sin\delta\,\cos(A_\circ + \Omega t - \alpha)$$

$$\left.+\,\Delta\delta\,\sin D\,\cos\delta + O(\Delta\alpha\Delta\delta)\right] + \Delta\phi_{\rm cyc}(t) + \Delta\phi_{\rm prop}(t) \tag{1a}$$

where $\Delta\phi_{\rm cyc} = 2\pi n^{'}$ is the phase difference due to the intrinsic cycle ambiguity of phase observables, and $\Delta\phi_{\rm prop}$ is the phase difference due to propagation effects along two different lines of sight, due to contributions from tropospheric and ionospheric fluctuations at X-band.

Phase delay is given by the ratio of the observed fringe phase and the reference angular frequency:

$$\tau_\phi = \frac{\phi(t)}{2\pi\nu} + \frac{n}{\nu} \tag{2}$$

where we have explicitly stated the inherent cycle ambiguity associated with the phase observable, which amounts to a phase delay ambiguity that is inversely proportional to the observing frequency. At an observing frequency of 8.4 GHz, the cycle ambiguity in delay amounts to integer multiples of ∼120 ps. To remove these ambiguities, we have used a phase connection technique that is described below.

Astrometric measurements provide two more observables in addition to the phase delay: the group delay and the phase delay rate (sometimes referred to as the delay rate for short). The group delay is given by

$$\tau_g = \frac{1}{2\pi}\frac{\partial\phi(t)}{\partial\nu} \tag{3}$$

The delay rate is the time derivative of the phase delay and is given by

$$\dot{\tau_\phi} = \frac{1}{2\pi\nu}\frac{\partial\phi(t)}{\partial t} \tag{4}$$

Unlike the phase delay observable, both group delay and delay rate observables are free of integer cycle ambiguities.

The error associated with a phase delay measurement (considering thermal error alone) is given by

$$\sigma_{\tau_\phi} = \frac{T_{\rm sys}}{2\pi\nu\,T_A\,\sqrt{n_p\,{\rm BW}\,\tau}} \tag{5}$$

where $T_{\rm sys}$ and T_A are the system and antenna temperature, respectively, n_p is the number of polarization channels recorded, BW is the recorded bandwidth, and τ is the integration time. A similar relationship can be obtained for errors associated with the group delay and delay rate observables. In the case of the group delay, the observing frequency ν is replaced with $\Delta\nu_{\rm rms}$, the root-mean-square of the spanned bandwidth, which is approximately given by $\Delta\nu/\sqrt{12}$, e.g., see [9]. Comparing the (thermal) errors for phase and group delay observables, with similar recording bandwidths, numbers of polarization channels, and integration times, the ratio of the errors is given by

$$\frac{\sigma_{\tau_\phi}}{\sigma_{\tau_G}} = \frac{\Delta\nu_{\rm rms}}{\nu} \tag{6}$$

where $\Delta\nu_{\rm rms}$ is the rms bandwidth for the group delay observable (for a pair of channels at the edges of the observing bandwidth, the rms bandwidth is 50 percent of the bandwidth). From this relationship, we observe that the typical gain in precision from a phase delay observable is a factor of >150 using a recording system similar to the VLBI Science Receiver (VSR) used in the DSN. (The VSR records a bandwidth of ∼100 MHz and has a maximum recording rate of 80 Mb/s.) Therefore, phase delay observables provide far better precision if measurement errors are predominantly due to thermal noise. However, as discussed above, fringe cycle ambiguities will need to be resolved in the case of phase delay observables.

III. Error Budget

The total error budget of spacecraft angular positions determined using the delta differential one-way ranging(ΔDOR)[2] [2] technique has been well established by a long series of successful measurements for a variety of spacecraft and observing geometries. The current ΔDOR error budget (see the blue bars in Fig. 1) estimates a mean total error of 2.5 nanoradians (nrad) or 0.5 milliarcseconds (mas), equivalent to a delay error of 60 picoseconds (ps). This error budget assumes a typical ΔDOR spacecraft–quasar angular separation of 6 deg and a cycle time of 10 minutes per scan.

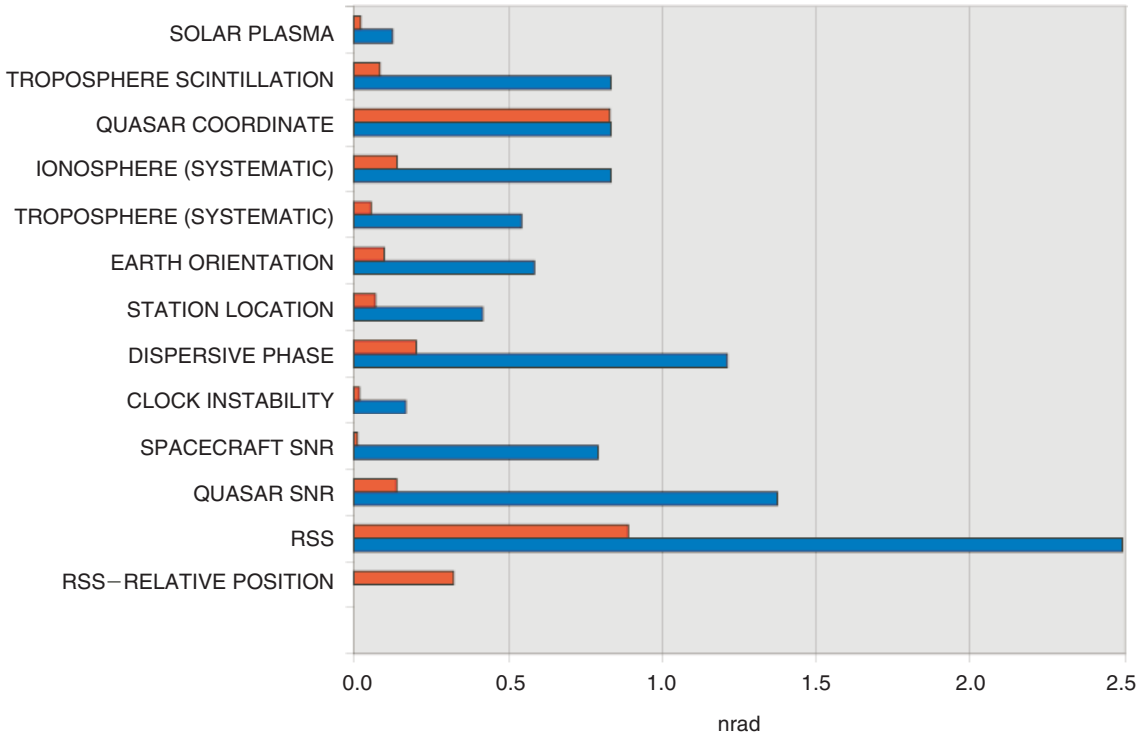

Fig. 1. The ΔDOR error budget at X-band with expected improvement: for each component, we have shown the current error estimates (blue) and the expected reduction in error (red) using techniques described in this article. Note that the quasar coordinate error is not affected by these techniques and remains at the present level in an absolute angular measurement.

[2] J. S. Border, "2004 Error Budget for DSN Delta Differential One-way Range Measurements," JPL Interoffice Memorandum 335-04-04-D (internal document), Jet Propulsion Laboratory, Pasadena, California, 2004.

By reducing both the angular separation between the quasar and the spacecraft as well as the temporal separation with fast cycle switching, we expect that many of the components in the total error budget will be reduced. Reducing both temporal and angular separation between reference and target source lines of sight will result in smaller differences in propagation effects due to solar plasma, tropospheric scintillation, and ionospheric fluctuations. Geometrical errors, such as those due to errors in Earth orientation parameters and station location, depend roughly linearly on reference-target angular separation. Therefore, these errors are expected to reduce linearly by a reduction in the angular separation. Station clocks are modeled linearly, and therefore reducing the temporal separation between the reference and target observation with faster switching cycles will reduce clock errors linearly with a scale factor determined by the ratio of reduction in the temporal separation.

Thermal errors, such as quasar and spacecraft SNR errors, can be reduced by using phase delay observables, as discussed earlier. However, the quasar SNR due to thermal noise will be improved by a factor of only 15, rather than the factor of 150 expected from using phase delays instead of group delay, since finding a quasar within 1 deg of the target necessarily requires the use of fainter (>50 mJy) radio sources than the typical reference quasar with a flux density of 0.5 Jy used for ΔDOR measurements.

Dispersive errors due to bandpass mismatch between narrow frequency channels spanning spacecraft signals and wider channels covering broadband quasar emission currently contribute a mean error of 1.25 nrad to the total group delay measurements of ΔDOR. One component of dispersive errors is temporal fluctuations of the bandpass, which can be reduced by using a faster switching time between observations of the reference and target sources. The remaining bandpass differences between narrow and wider channels can be reduced by applying bandpass calibration techniques in VLBI observations using bright calibrators. These techniques and the expected reduction in bandpass error will be discussed in a separate article. For the purpose of this discussion, we expect a linear reduction in dispersive errors due to a reduction in temporal separation.

Figure 1 also shows (in red) the expected error reduction by carrying out phase delay observations with a mean spacecraft–quasar angular separation of 1 deg and a temporal separation of 1 minute. We note that the quasar coordinate error (catalog error) is unaffected and remains at the 0.75-nrad level. It is expected that by going to 32 GHz (Ka-band) a catalog with a mean error of 0.5 nrad will be developed in the future.[3] Assuming error components are independent, we sum them in quadrature and obtain a total relative position error of $\sim$0.3 nrad. On the other hand, the total expected absolute position error is $\lesssim$0.9 nrad, dominated by catalog errors.

IV. Selection of Quasar Pairs

We selected quasar pairs from a catalog of sources [3] used to define the International Celestial Reference Frame (ICRF). This catalog contains $\sim$500 sources, which tend to be bright radio sources with compact cores. The pairs selected for observation were required to have an angular separation of 1 to 3 deg. The correlated flux density of each source is in the range of 0.15 to 0.6 Jy over a $\sim$5000 km baseline, as measured at the Very Long Baseline Array (VLBA). Each source also was required to be compact with minimal structure, and thus is treated as a point source in the subsequent analysis.

Table 1 lists the properties of the observed pairs, including source coordinates in right ascension and declination, 8-GHz correlated flux density, and the pair's angular separation.

[3] C. Jacobs, personal communication, Jet Propulsion Laboratory, Pasadena, California, 2007.

Table 1. List of quasar pairs observed at the DSN. Quasar coordinates in right ascension and declination are provided for the J2000 epoch, and the formal errors are reported in parentheses. $\Delta\theta$ refers to angular separation of the two quasars; flux density refers to the correlated flux density at a ∼5000 km baseline at 8 GHz, obtained at the VLBA (1994-2005); and (c) indicates the reference or calibrator quasar.

Pair	Name	Right ascension (α)	Declination (δ)	Flux, Jy	$\Delta\theta$, deg
1	0159+723 (c)	$02^{\rm h}03^{\rm m}33^{\rm s}.384999(12)$	$72°32'53''.66731(5)$	0.12	2.2
	0153+744	$01^{\rm h}57^{\rm m}34^{\rm s}.965097(30)$	$74°42'43''.22994(14)$	0.14	
2	0805+410 (c)	$08^{\rm h}08^{\rm m}56^{\rm s}.652039(1)$	$40°52'44''.88881(1)$	0.56	2.3
	0814+425	$08^{\rm h}18^{\rm m}15^{\rm s}.999605(8)$	$42°22'45''.41497(14)$	0.55	
3	1030+415 (c)	$10^{\rm h}33^{\rm m}03^{\rm s}.707860(3)$	$41°16'06''.23290(5)$	0.57	2.4
	1020+400	$10^{\rm h}23^{\rm m}11^{\rm s}.565652(2)$	$39°48'15''.38535(4)$	0.48	
4	1044+719 (c)	$10^{\rm h}48^{\rm m}27^{\rm s}.619897(1)$	$71°43'35''.93831(1)$	0.65	1.7
	1053+704	$10^{\rm h}56^{\rm m}53^{\rm s}.617491(4)$	$70°11'45''.91560(2)$	0.35	
5	1849+670 (c)	$18^{\rm h}49^{\rm m}16^{\rm s}.072281(2)$	$67°05'41''.68048(1)$	0.53	1.2
	1842+681	$18^{\rm h}42^{\rm m}33^{\rm s}.641688(4)$	$68°09'25''.22796(2)$	0.44	

V. Observations

We have carried out a number of VLBI observations of pairs of quasars with the DSN 34-m antennas over the course of a year and a half. Results reported in this article are obtained from two X-band observing sessions. Table 2 lists observation dates, durations, antennas, observed frequencies, and spanned bandwidths of the back-end recording device.

Each observing session lasted roughly 4 hours, during which 3 pairs were observed. The first session was carried out in December 2005 using DSS-24 and DSS-54 antennas on the ∼8400 km California–Spain baseline. The VSR was used to carry out the recording using 4 Nyquist 2-bit-sampled channels, each 2-MHz wide over a spanned bandwidth of 66 MHz. Each pair was observed for 1 to 1.5 hours, with a cycle time of 2.5 minutes. Right-circular polarization was recorded during each session. The second session was carried out almost a year later in December 2006 on a similar baseline using DSS-25 and DSS-55 antennas. For this experiment, the wideband VSR (WVSR), spanning 380 MHz, was available at each station and was used to obtain better group delay estimates. Unfortunately, the recording rate of the WVSR is still limited to 80 Mb/s, similar to the VSR, and therefore it does not improve detection sensitivity. For this experiment, we used a shorter cycle time of 1 to 1.5 minutes between the sources. In addition to observing the pairs of quasars, a number of bright calibrators were also observed in each session over a 15- to 30-minute period in order to obtain an estimate for the zenith troposphere delay.

Table 2. VLBI Observations at the DSN.

Date	Duration, hr	DSN baseline	Cycle time, min	Channels	Spanned bandwidth, MHz
December 10, 2005	4	24–54	2.5	4	66
October 6, 2006	4.5	25–55	1–1.5	5	380

VI. Data Analysis

Recorded channels from each antenna were cross-correlated using SOFTC, JPL's software correlator,[4] in four spectral bins per frequency channel, using an integration time of 1 second. A fringe search then was carried out for each scan, estimating group delay, phase delay, and the phase delay rate for each source at a nominal frequency, ν, that was slightly different for each observation epoch due to the different number of frequency channels recorded at each epoch. In subsequent analysis, one of the quasars was considered to be the nominal reference calibrator, as indicated in Table 1. Further post-fringe-fitting analysis of observables was carried out in MODEST [8].

A. Group Delay and Delay Rate Observables

The group delays and delay rates from each session, including observations of bright calibrators, were used in MODEST to estimate the initial clock parameters (offset and rate) and the zenith troposphere delay, while all other parameters, including source positions, baseline vector, and Earth orientation parameters, were held fixed. In further analysis, troposphere parameters were fixed at these values for each observing epoch.

For each observed pair, using group delay and delay rate measurements, we estimated the clock parameters and the angular position of the target source. The least-square analysis was carried out while holding the position of the calibrator fixed to its nominal a priori position, with formal error at the level of tens of microarcseconds.

The precision of the angular position measurement as obtained from the group delay observable is inversely proportional to the SNR of the measurements, which in turn depends on the flux density of the source. Using a variation of Eq. (5) for group delay observables, the requirement that $\sigma_{\tau_G} < 60$ ps can be stated as SNR $> 3000/\Delta\nu_{\rm rms}$ [MHz].

Using the VSR, with a bandwidth of about 100 MHz (effective bandwidth $\Delta\nu_{\rm rms} \sim 50$ MHz), large values of SNR (>180) are required in order to obtain position error at the level of half a fringe cycle (3σ). The WVSR improves the SNR requirement somewhat to >40. The high values of SNR required to carry out these observations in turn limits these measurements to targets with brightness above a certain flux density. Given a pair of 34-m antennas, system temperatures of 30 K, integration times of 2 minutes, and a maximum recording rate of 40 Mb/s (available with either the VSR or the WVSR), group delay measurements can be carried out with the stated precision for sources with a flux density above ∼200 and ∼40 mJy, using the VSR and the WVSR, respectively. For comparison, the Mark5 recorder with a recording rate of 1 gigabit per second (Gbps) and a bandwidth of 500 MHz will allow for group delay measurements with a precision of $\sigma_{\tau_G} < 60$ ps for sources with a flux greater than ∼20 mJy. We note that, while for our observations these requirements must be met for both target and calibrator sources, in the case of applying these techniques to measuring the angular position of a spacecraft, only the calibrator needs to be sufficiently bright to obtain the stated SNR in its group delay observable. Typically, the spacecraft signal (DOR tones) provides much higher SNR than do the natural radio sources used as calibrators, and therefore this stringent requirement is met more easily when the target is a spacecraft.

B. Phase Connection

Before seeking a phase delay solution, it is assumed that the position of the target is known to within a delay beam, $c/(\Delta\nu B)$, or a few arcseconds. In our case, the quasar positions are known to submilliarcsecond accuracy. In the case of spacecraft measurements, Doppler measurements already determine angular position at this level.

[4] S. T. Lowe, "SOFTC: A Software VLBI Correlator," JPL internal document, Jet Propulsion Laboratory, Pasadena, California, 2003.

Then, the position of the target is determined within a fringe phase cycle, using either group delay measurements for bright quasars in these measurements or the approach discussed in [1]. We then proceeded with the phase delay solution using the least-square MODEST package to obtain precision source-position estimates for the target. In this phase of the analysis, we once again hold the calibrator position fixed to its nominal position. In addition, the troposphere parameters are also held fixed to the previously obtained global solution (using all observations during the epoch, including those of other bright calibrators). The a priori position for the target source is set to the values obtained previously with the group delay solution. We also allow the clock parameters (clock offset and rate) to be estimated by MODEST for reasons that will be discussed further below.

Before proceeding with a least-square analysis in MODEST, phases for both calibrator and target source are unwrapped. In this step, the o-c (observed minus calculated) residual phase for each scan is examined for shifts of greater than one-half a cycle from neighboring scans, and ±1 cycle (∼120 ps at X-band) is added to the phase solution to unwrap phase jumps, resolving any cycle ambiguities. Once phase unwrapping is carried out, calibrator phases are used in a least-square solution to obtain estimates of clock parameters. The clock parameters then are held fixed at these values, and phase residuals of the target source are obtained from a least-square analysis. As an example, Fig. 2 illustrates the above process for the (1044+719, 1053+704) pair observed in October 2006.

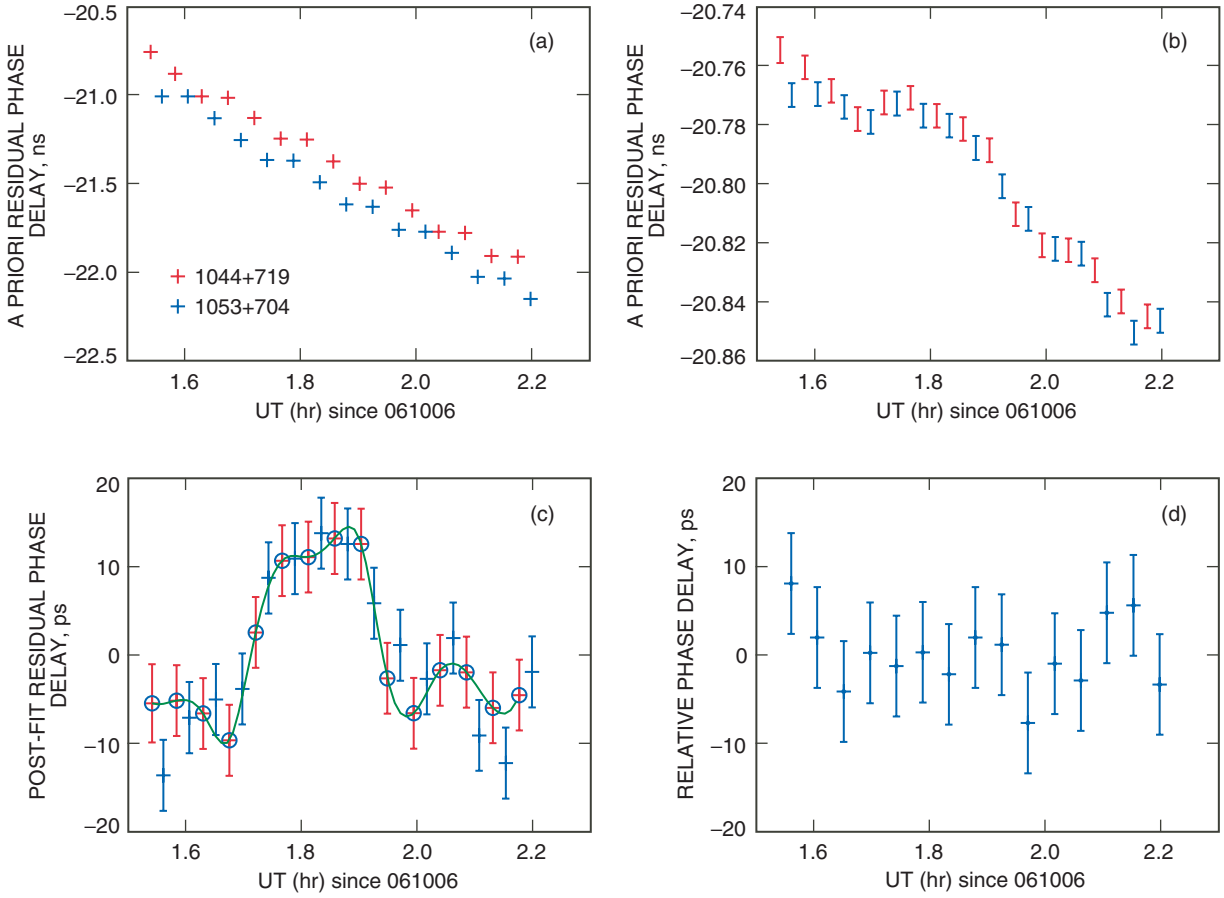

Fig. 2. Phase delay solution of 1044+719 (calibrator) and 1053+704 (target) observed at 8.4 GHz on October 6, 2006, at DSS 25 and DSS 55: (a) a priori o-c phase residuals using model values described in the text with no attempt at cycle ambiguity resolution, (b) a priori phase residuals after cycle ambiguity resolution as described in the text, (c) post-fit residuals after solving for target position and clock parameters, and (d) relative phase delay residuals after interpolated calibrator solutions are subtracted from the target observables. The rms of the phase delay residual in this case has been reduced to 4 ps, corresponding to an angular position error of 30 microarcseconds (0.15 nrad).

In the next stage, we interpolated the phase residuals of the calibrator, using a piecewise cubic interpolation algorithm to obtain phase residual values at the reference times of target scans. The differences between the calibrator-interpolated values and the target phase residuals provide a measure of the precision of the relative astrometry achieved in each observation. This difference cancels a large fraction of the fluctuations due to propagation error and of the errors in observing geometry, achieving a resolution limited largely by thermal noise. In the case of this particular observation, Fig. 2(d), the relative phase delay residuals have an rms of 4 ps, equivalent to an angular position error of 30 μas (0.15 nrad).

Our solutions were able to differentiate incorrect cycle ambiguity resolution. Figure 3 illustrates a solution for the same pair of sources, where at 16 minutes past the start of the observations a cycle is deliberately added to the target observable. As evident in the figure, the incorrect cycle assignment greatly degrades the rms of the relative phase delay residuals to 30 ps (factor of 5) and is very obvious. Removing this scan from the solutions improves the relative residuals to 6 ps.

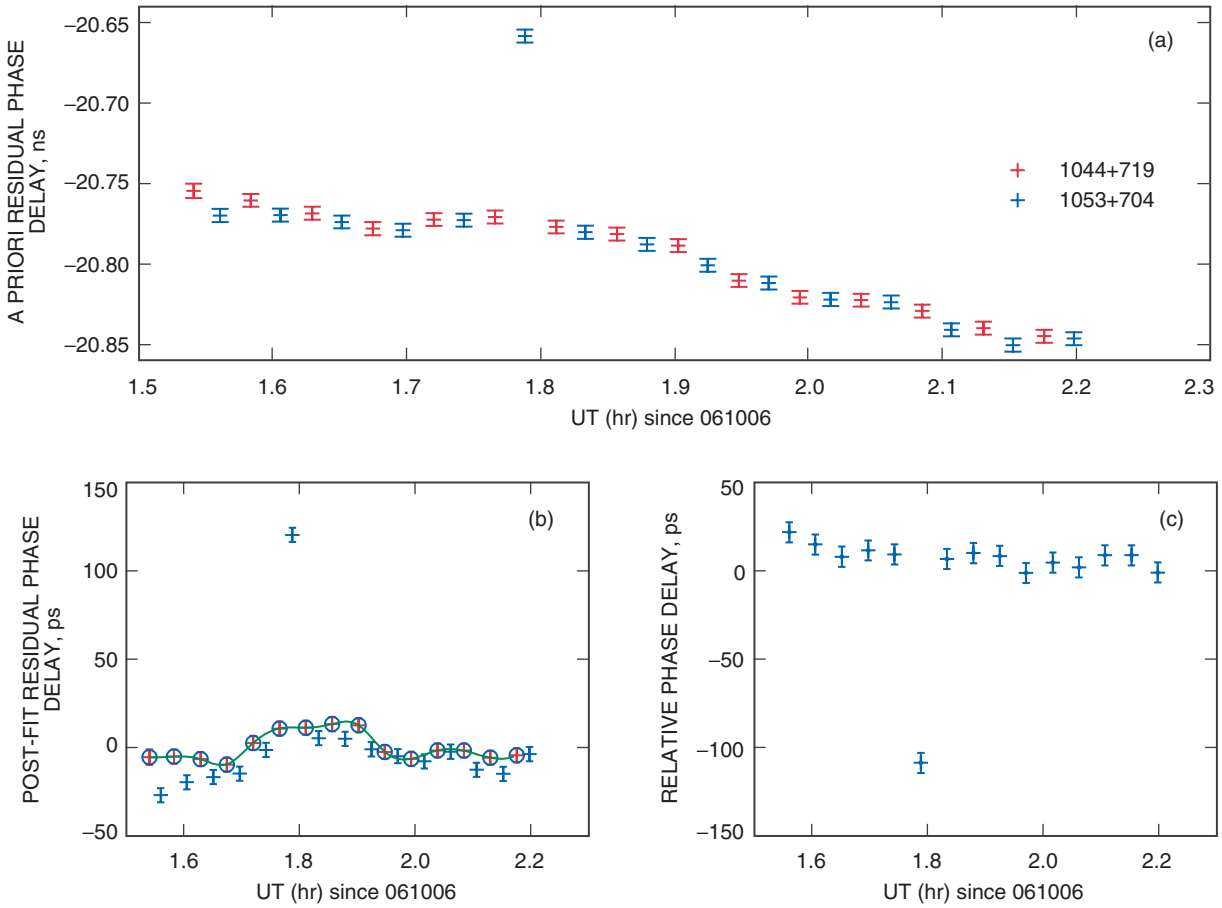

Fig. 3. Introducing an intentional cycle jump in the phase delay solution of 1044+719 (calibrator) and 1053+704 (target) observed at 8.4 GHz on October 6, 2006: (a) a priori phase residuals after cycle ambiguity resolution and the deliberate addition of a cycle after 16 minutes of observations, (b) post-fit residuals after solving for target position and clock parameters, and (c) relative phase delay residuals after interpolated calibrator solutions are subtracted from target observables. The rms of the phase residuals is now 30 ps. If the offending scan is removed, the rms improves to 6 ps.

C. Clock Parameters

We used two parameters, a dc offset and a rate, to model the clock. As noted above, we allowed the clock parameters in the phase delay least-square solution to be different from those estimated in the group delay solution. In fact, our observations during the two epochs show large differences between the clock dc term of the group and phase delay solutions. These differences are about 80 ns for the December 2005 session on the DSS 24–DSS 54 baseline and about 20 ns for the October 2006 session on the DSS 25–DSS 55 baseline. On any given day, however, the difference in the dc term as obtained in the independent analysis for each pair is at the nanosecond level, perhaps indicative of tropospheric and ionospheric changes over the length of the observing epoch. The clock rates, on the other hand, differ at the level of a few times 10^{-14} s/s. In this section, we will discuss our approach and reasons why the clock-like contribution to the two delay observables may be quite different.

There are arbitrary, but typically constant, delay offsets between a group delay measurement and a phase delay measurement. The group delay measurement is carried out using a bandwidth synthesis (BWS) approach [6], which uses the difference in the phase of multiple frequency channels ($\tau_{gd} \propto \partial\phi/\partial\nu$) to obtain a group delay measurement. The group delay, therefore, removes any common-mode delay component among the channels. The phase delay observable, on the other hand, is obtained directly from measurement of the phase at a given frequency, which may not remove any common-mode delay offsets among channels.

In addition, any dispersive component of the delay in the form of ν^{-n}, where n is a positive real number, will contribute to the group delay and phase delay with opposite signs. Both instrumental and ionospheric errors are examples exhibiting dispersive behavior.

For instance, the delay of a radio wave propagating through Earth's ionosphere is approximated by [7]

$$\Delta\tau_{\rm iono} = \pm k\, E_c/\nu^2 \tag{7}$$

where $k \simeq 1.34 \times 10^{-7}$ m^{2}s^{-3}, E_c is the integrated electron content [m^{-2}] and ν is the observing frequency [Hz]. The plus/minus signs refer to the change in sign for group and phase delays, respectively. Since we are not modeling the ionosphere, and therefore have no way to estimate the contribution due to the ionosphere, the group delay and the phase delays are expected to differ by twice the absolute value of the above term. The constant as well as any linear drift in the delay due to the ionosphere also will be absorbed in the clock offset and rate terms.

On the other hand, any fluctuations of ionospheric delay (beyond dc and linear drift terms) will adversely affect the precision of the measurement. However, a large part of that should cancel out due to common mode rejection between the calibrator and the target source. Fortunately, our observations were made in a period of low solar activity and therefore we also don't expect the fluctuations (beyond the linear term) to be large.

As an example, we consider the observation of the 1044+719, 1053+704 pair in 2006. We broke up the 1-hour observation into three periods, roughly comparable in length, and carried out a similar least-square analysis. We attempted to model the clock in a piecewise fashion, covering the roughly 1-hour observation with three adjacent epochs, each about 1,200 s long. While we held the clock rate fixed at the previously estimated value, we obtained three new estimates for the clock dc-offset term. These values differed from the nominal offset values by 1, 8, and 2 ps for each of the successive epochs. Similarly, we held the clock offset term fixed and estimated a rate for each period. The estimated values were $(0.6, 1.1, 1.0) \times 10^{-15}$ s/s. The maximum delay error due to the drift rate is then 1.2 ps.

D. Relative Group Delay Observables

We also looked at difference observables of group delays in a fashion similar to the above discussion of phase delay observables. Since there is no need to resolve cycle ambiguities in this case, we proceeded by differencing the interpolated calibrator delay observable with the corresponding target observable. Figure 4 shows an example of the relative group delay observables for the same pair as shown in Figs. 2 and 3. The scatter in the group delay residuals for either source is ∼25 ps, much improved because of the wideband recording capability of the WVSR. This is roughly a factor of 5 improvement over similar measurements recorded with the VSR. The difference observables in this case do not yield improved precision, because the intrinsic scatter of the observables is comparable to the measurement errors.

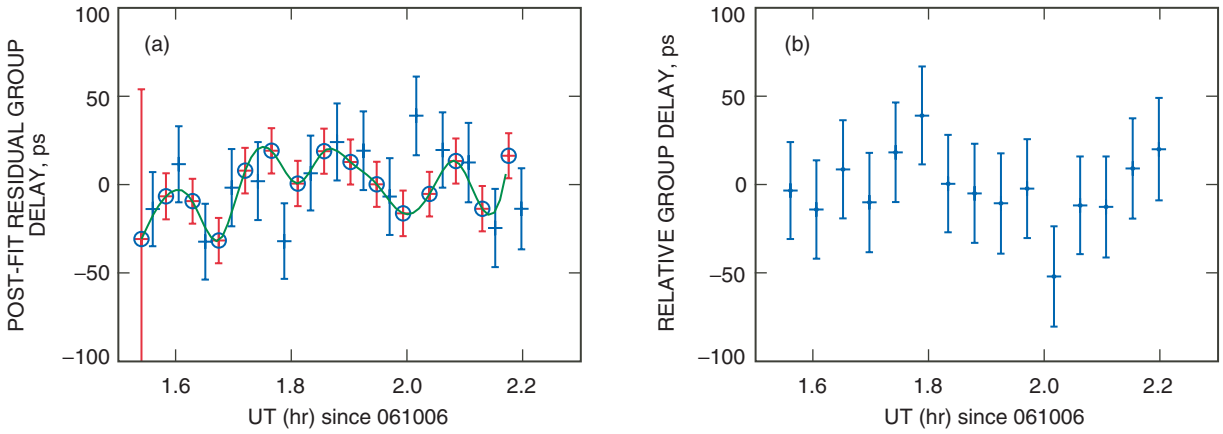

Fig. 4. Difference group delay observables of 1044+719 (calibrator) and 1053+704 (target) observed at 8.4 GHz on October 6, 2006: (a) post-fit residuals after solving for target position and clock parameters and (b) relative group delay residuals after interpolated calibrator solutions are subtracted from target observables. The rms of the difference observables in this case does not improve due to the large scatter of the group delay observables (~25 ps).

VII. Results

The analysis procedure outlined above was successfully applied for all observed pairs during both epochs of observations (see Figs. 2, 4, and 5 through 9). Table 3 shows results from both relative phase and relative group delay solutions for each pair. Phase delay residuals are all at the level of a few picoseconds, while group delay residuals are much worse, as expected. The large group delay error is dominated by thermal noise, indicating that group delay errors are flux limited at this level.

We point out, however, that group delay errors even as large as 100 ps have no detrimental effect on the precision and accuracy of phase delay solutions. We have carried out a number of tests where the a priori position of the target source is moved in both right ascension and declination by 5 to 15 nrad from the estimated group delay position. The results show that, even with such large deviations from the correct group delay solution, the phase delay estimate converges back to the same position as the initial phase solution obtained from the nominal a priori position obtained from group delay position. Our tests show that the convergence error is within ∼0.1 nrad of the initial position. The fact that phase observables are not very sensitive to group delay a prioris, shows great promise that fainter sources, and thus nearby (in angle) to target source, calibrators can be used to obtain a group delay solution with less stringent accuracy than is normally expected of accurate ΔDOR measurements. A full description of this technique and its implications is discussed elsewhere [1].

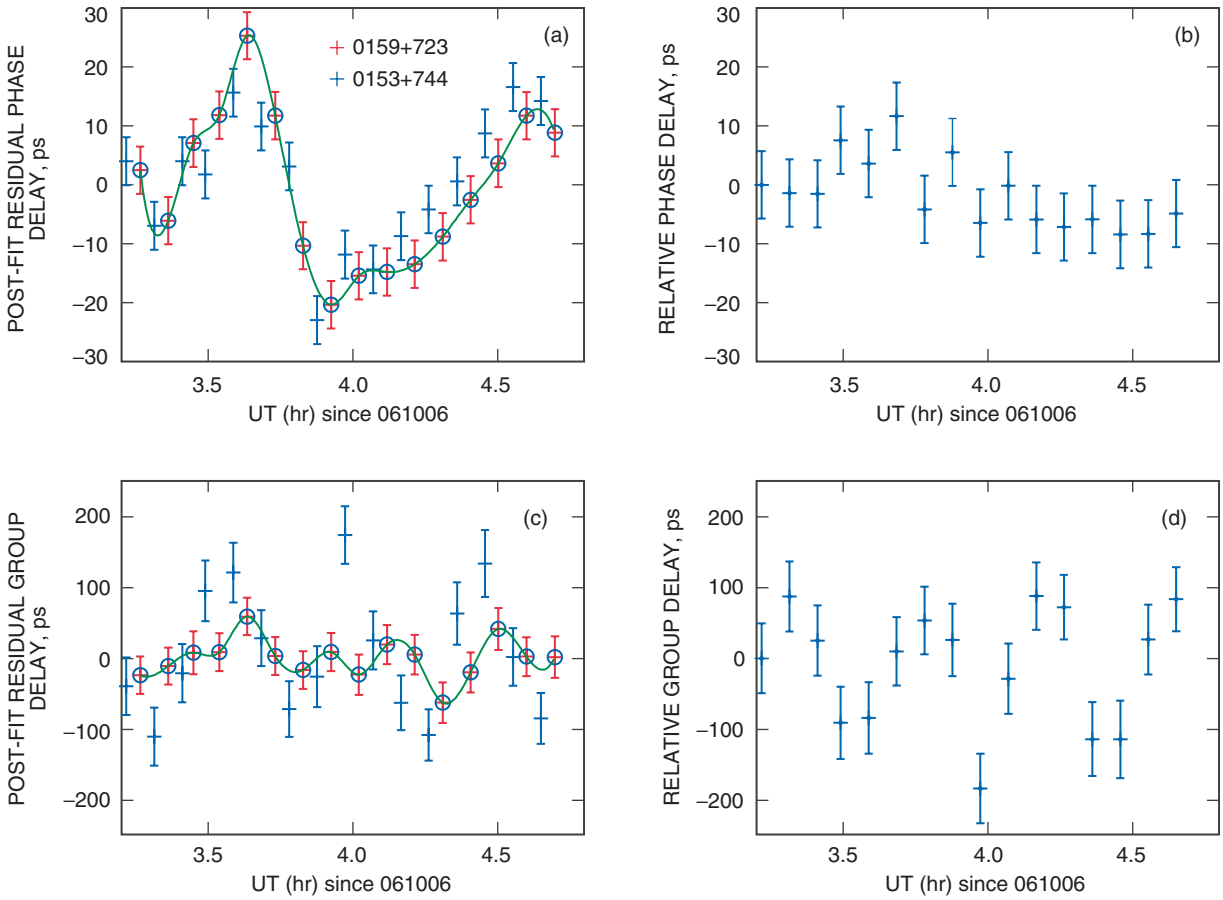

Fig. 5. Comparison of phase and group delay observables for 0159+723 (calibrator) and 0153+744 (target) observed at 8.4 GHz on October 6, 2006: (a) post-fit phase delay residuals, (b) relative phase delay residuals yielding an rms of 6 ps, (c) post-fit group delay residuals, and (d) relative group delay residuals yielding an rms of 85 ps.

VIII. Discussion

Our pilot measurements show that reducing both the angular and temporal separations between calibrator and target, and the use of phase delay observables, can greatly improve the measurement of relative angular position of the target with respect to the calibrator position. A rough estimate of the target position was first obtained from calibrated group delay observables. In some cases, group delay errors were large, due to either inadequate bandwidth or low flux density. However, in all cases we were able to successfully connect phase and obtain phase delay errors at the level of a few picoseconds, equivalent to $\sim$0.2 nrad precision in the plane-of-sky angle measurement.

We expect that, in the case where the target is a spacecraft, similar precision will be obtained in determining the angular position of the spacecraft [1]. Since spacecraft signals are not broadband like natural radio sources, either DOR tones or telemetry signals can be used to carry out VLBI measurements. For a spacecraft tone, the SNR (in 1 second of integration) is related to $P_{\rm tone}/N_{\circ}$, the tone-to-noise power ratio in a 1-Hz bandwidth, by SNR $\sim \sqrt{P_{\rm tone}/N_{\circ}}$. The ΔDOR error budget assumes a 20 dB-Hz signal, equivalent to a 1-second SNR of 100. Using an integration time of 1 minute and both DOR tones yields an effective SNR of >500, which results in a thermal noise error of a few picoseconds. In the case of 8-MHz telemetry, while the bandwidth is narrower, the SNR is much larger due to the large number of bits (even with a 0-dB/bit signal and 4 Mb/s, the SNR is large).

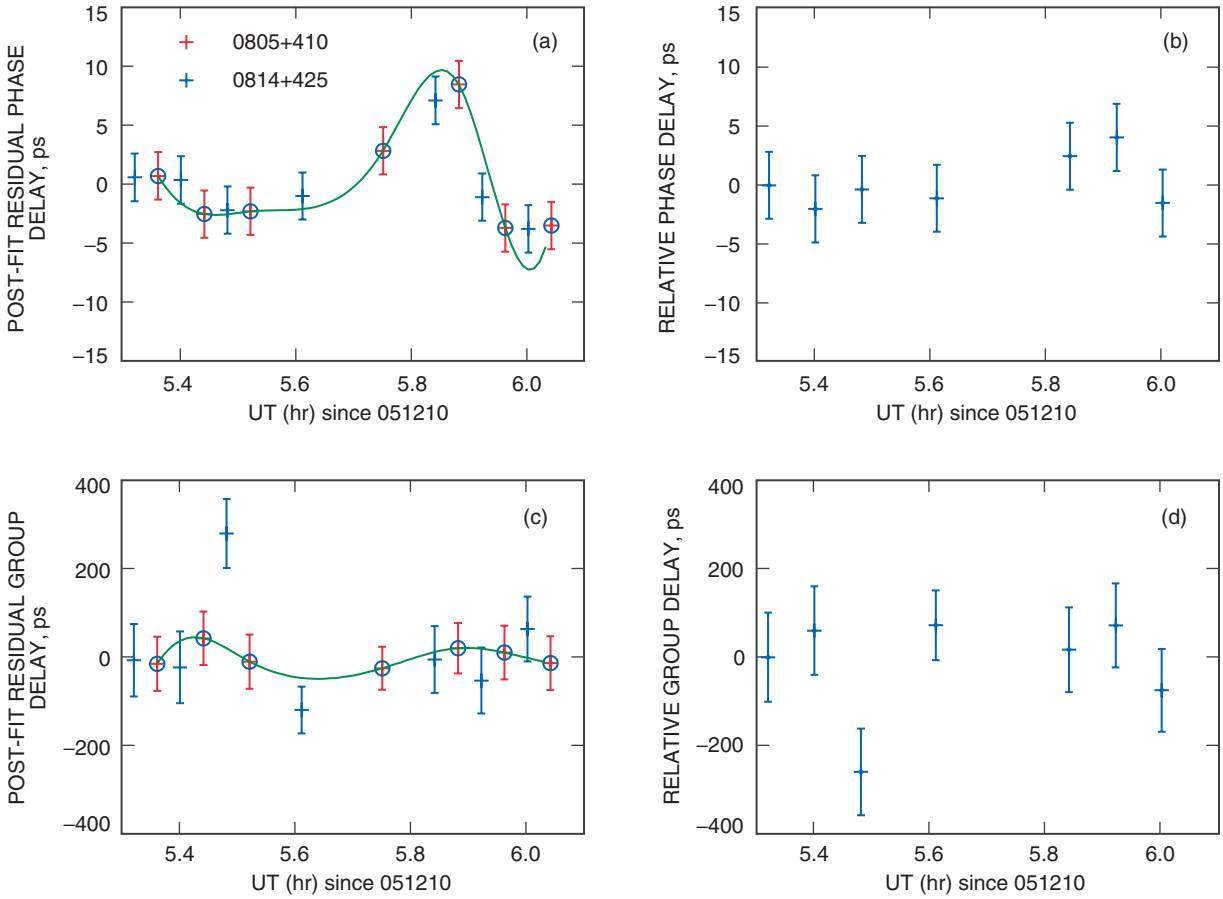

Fig. 6. Comparison of phase and group delay observables for 0805+410 (calibrator) and 0814+425 (target) observed at 8.4 GHz on December 10, 2005: (a) post-fit phase delay residuals, (b) relative phase delay residuals yielding an rms of 3 ps, (c) post-fit group delay residuals, and (d) relative group delay residuals yielding an rms of 120 ps.

The one-sigma flux detection sensitivity with a pair of 34-m antennas, each with a system temperature of 30 K and an integration time of 1 minute, is roughly 6 mJy with a recording bandwidth of 10 Mb/s (typical of the VSR/WVSR). In the case of the Mark5 recording system, the sensitivity is improved by a factor of almost 8 to 0.75 mJy. Requiring an SNR of 5 (∼10 deg of phase error), the detection threshold is 30 mJy with the VSR/WVSR and 4 mJy with the Mark5 recording system.

Source count studies [4,5] at 30/4 mJy suggest 1.2/19.4 sources per square degree. With a probability of ∼30 percent that these sources contain compact cores, we expect 0.36/5.8 compact sources per square degree, which is equivalent to a mean angular distance of 0.9/0.2 deg to a compact source.

Based on results discussed in this article, we think it may be possible to improve the accuracy of relative spacecraft angular position measurements to a level of ∼1/3 nrad, using calibrators as weak as 50 mJy. We note, however, that absolute position measurements will need to take into account the error associated with the calibrator position, which is related to an astrometric catalog error of 0.75 nrad at X-band. In addition, we have not made an attempt to estimate errors due to source (calibrator) structure. We do, however, expect that source structure errors for faint sources will decrease due to synchrotron self-absorption. Studies are needed to examine and quantify source structure effects. In addition, further observations are necessary to study the robustness of the techniques discussed in this article and to demonstrate the validity of this approach for spacecraft tracking using a spacecraft as the target source.

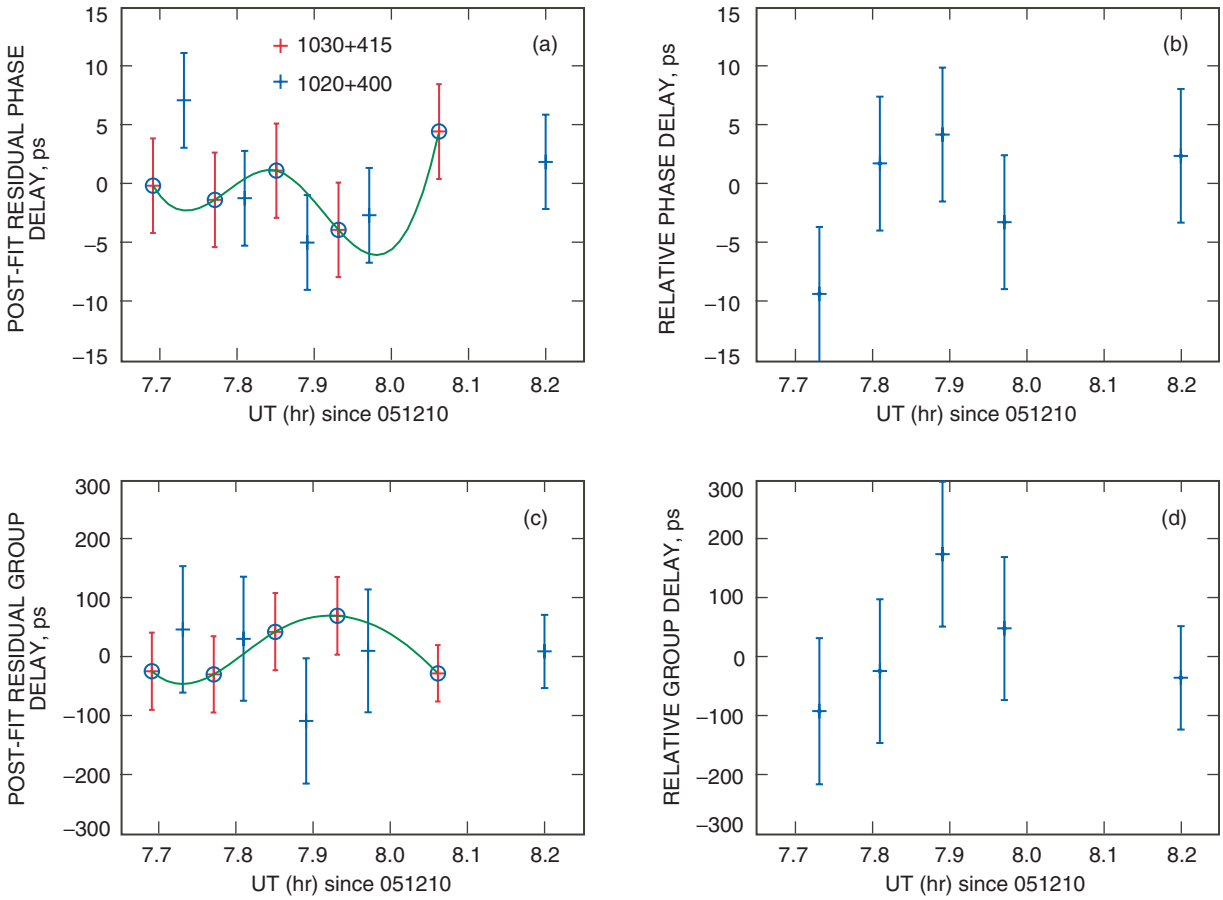

Fig. 7. Comparison of phase and group delay observables for 1030+415 (calibrator) and 1020+400 (target) observed at 8.4 GHz on December 10, 2005: (a) post-fit phase delay residuals, (b) relative phase delay residuals yielding an rms of 6 ps, (c) post-fit group delay residuals, and (d) relative group delay residuals yielding an rms of 102 ps.

IX. Conclusions

We have described results from pilot VLBI observations at the DSN of pairs of nearby (in angle) quasar pairs at a frequency of 8.4 GHz. We have employed a fast-switching technique, switching between calibrator and target source, with cycle times of 1 to 2 minutes. By reducing both the temporal and angular separations between the calibrator and target source, we have minimized calibration errors due to both media propagation effects as well as geometric effects. We have also used phase delay observables to improve astrometric precision and have described a method for phase connection. Error budget estimates indicate that relative astrometric accuracy at the level of 1/3 nrad may be achieved by using calibrators within 1 deg of the target source. Absolute measurement accuracy will also be affected by the error in the calibrator position, which currently can be obtained at the level of 0.75 nrad. Future catalog improvements may result in 0.5-nrad catalog error. To demonstrate the robustness of this approach, we plan to carry out further VLBI observations of quasar pairs. In addition, we hope to carry out similar observations with spacecraft as the target sources to further validate the estimated error budget provided here.

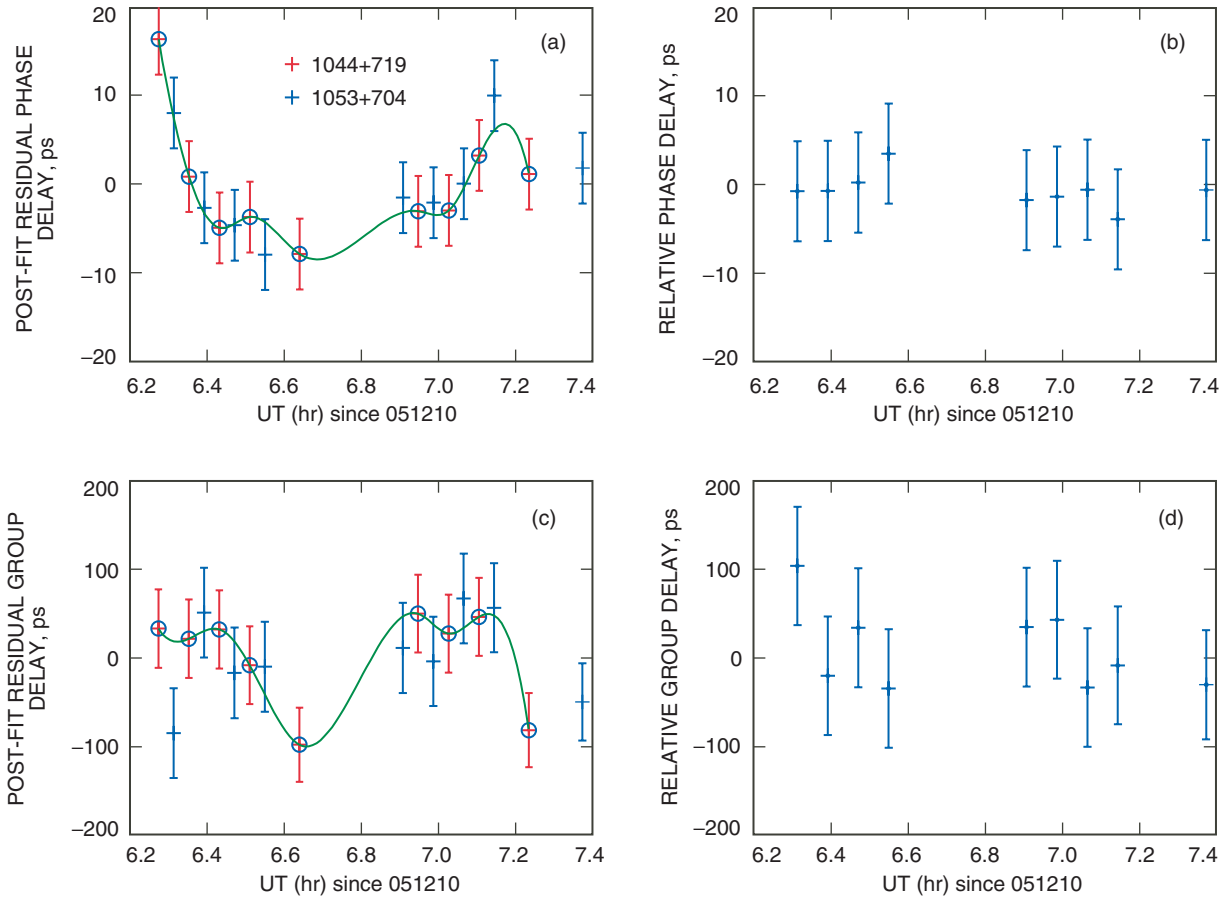

Fig. 8. Comparison of phase and group delay observables for 1044+719 (calibrator) and 1053+704 (target) observed at 8.4 GHz on December 10, 2005: (a) post-fit phase delay residuals, (b) relative phase delay residuals yielding an rms of 3 ps, (c) post-fit group delay residuals, and (d) relative group delay residuals yielding an rms of 48 ps.

Acknowledgments

We would like to express out thanks and gratitude to the staff of the DSN complexes at Goldstone and Madrid, in particular Lyle Skjerve at Goldstone, who helped us carry out pilot observations at DSS 13, and Cristina Garcia Miro in Madrid for her assistance in carrying out these observations. We thank Gabor Lanyi and Chris Jacobs for helpful discussions about MODEST. The authors also express their thanks to the referee, Dayton Jones, for his careful reading of the manuscript and helpful comments.

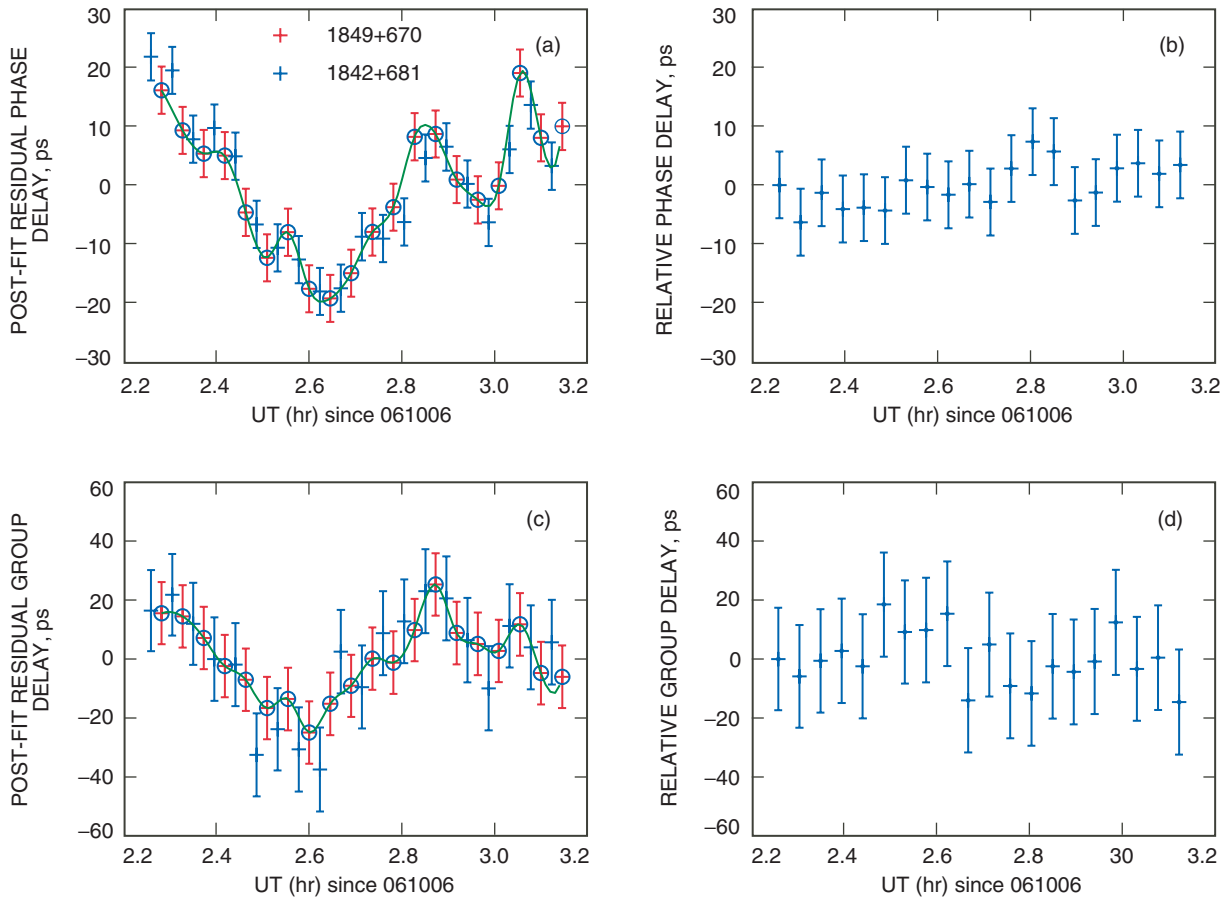

Fig. 9. Comparison of phase and group delay observables for 1849+670 (calibrator) and 1842+681 (target) observed at 8.4 GHz on October 6, 2006: (a) post-fit phase delay residuals, (b) relative phase delay residuals yielding an rms of 3.6 ps, (c) post-fit group delay residuals, and (d) relative group delay residuals yielding an rms of 9.3 ps.

Table 3. Results of difference observables for phase and group delay after the least-square analysis described in the text.

Target	Calibrator	Angular separation, deg	Epoch	Phase delay residual, ps	Group delay residual, ps	Figure number
0153+744	0159+723	2.2	October 2006	6	85	5
0814+425	0805+410	2.3	December 2005	3	120	6
1020+400	1030+415	2.4	December 2005	6	102	7
1053+704	1044+719	1.7	December 2005	3	48	8
1053+704	1044+719	1.7	October 2006	4	20	2,4
1842+681	1849+670	1.2	October 2006	4	9	9

References

[1] D. S. Bagri and W. A. Majid, "Estimating Accurate Relative Spacecraft Angular Position from Deep Space Network Very Long Baseline Interferometry Phases Using X-band Telemetry or Differential One-Way Ranging Tones," *The Interplanetary Network Progress Report*, vol. 42-172, Jet Propulsion Laboratory, Pasadena, California, pp. 1–10, February 15, 2007.
http://ipnpr/progress_report/42-172/172B.pdf

[2] G. Lanyi, D. Bagri, and J. Border, "Angular Position Determination of Spacecraft by Radio Interferometry," *Proceedings of the IEEE*, vol. 95, no. 11, 2007 (in press).

[3] A. L. Fey, C. Ma, E. F. Arias, P. Charlot, M. Feissel-Vernier, A. M. Gontier, C. S. Jacobs, J. Li, and D. S. MacMillan, "The Second Extension of the International Celestial Reference Frame: ICRF-EXT.1," *The Astronomical Journal*, vol. 127, pp. 3587–3608, June 2004.

[4] B. Henkel and R. B. Partridge, "Completing the Counts of Radio Sources at 8.5 GHz," *The Astrophysical Journal*, vol. 635, pp. 950–958, 2005.

[5] W. Majid and D. Bagri, "In-Beam Phase Referencing with the Deep Space Network Array," *The Interplanetary Network Progress Report*, vol. 42-169, Jet Propulsion Laboratory, Pasadena, California, pp. 1–7, May 15, 2007.
http://ipnpr/progress_report/42-169/169F.pdf

[6] A. E. E. Rogers, "VLBI with Large Effective Bandwidth for Phase Delay Measurements," *Radio Science*, vol. 5, pp. 1239–1247, 1970.

[7] J. S. Sovers, J. L. Fanselow, and C. S. Jacobs, "Astrometry and Geodesy with Radio Interferometry: Experiments, Models, Results," *Rev. Mod. Phys.*, vol. 70, pp. 1393–1454, 1998.

[8] O. J. Sovers and C. S. Jacobs, *Observation Model and Parameter Partials for JPL VLBI Parameter Estimation Software MODEST*, JPL Publication 83-39, Rev. 6, Jet Propulsion Laboratory, Pasadena, California, August 1996.

[9] A. R. Thompson, J. M. Moran, and G. W. Swenson, *Interferometry and Synthesis in Radio Astronomy*, New York: John Wiley and Sons, Inc., 2001.